3. Introduction

Bioactive glasses (BGs) are bio and cytocompatible third-generation silica-based inorganic compounds that have tremendous tissue regenerative potential (Majumdar, Gupta et al. 2022) and are mostly used as implants or as drug delivery systems due to their mesoporous nature (Gupta, Majumdar et al. 2021). Their bioactivity is attributed to the various therapeutic dopants present in its silica network that are leached into the physiological environment (Majumdar, Gupta et al. 2021, Taye 2022) which activates a cascade of proteins or ion channels required for physiological activity. Recently, the pharmacological efficacy of BGs has also been explored and the orally administered barium-doped BG (BaBG) exhibited an anti-ulcer effect in various gastric ulcer models in rats (Paliwal, Kumar et al. 2018). Therefore, the clinical translation for systemic use necessitates investigating the release kinetic profile and biodistribution of the dopants leached from BGs. Further, due to the inherent osteogenic and bactericidal properties, BGs are used clinically as orthopedic implants for extremely serious orthopedic deformities (Schepers, Ducheyne et al. 1993, Jones, Brauer et al. 2016). The clinical implants for osseous tissues are required to be present *in situ* throughout the patient's life. So, these implants must have higher stability with a low leaching tendency. Hence, determining the preclinical release kinetic profile of the dopants of BGs will confer light on their chemical and biological stability when used as implants.

In general, the therapeutic ions that are doped in the silica network of BGs are an integral part of the normal physiology of the body where the ionic homeostasis is maintained (Majumdar, Gupta et al. 2021). These physiologically and pharmacologically active dopants produce therapeutic efficacy if the leaching ionic concentrations are within the physiological limits. However, if this physiological ionic

set-point is broken due to excessive leaching of doped elements it may lead to various physiochemical, pharmacokinetic, and pharmacodynamic interactions (Rivadeneira, Luz et al. 2015, Zheng, Kapp et al. 2019). Additionally, the release of dopants from BGs causes an increase in the pH as described in **Chapter 1** which may alter the bioavailability of weak acidic drugs whose absorption is pH-dependent (Akula and PK 2018) and hence may affect their onset of action and bioavailability. Moreover, BGs may even cause increased accumulation of dopants in excretory organs which will change the *in situ* ionic homeostasis (Mao, Chen et al. 2016). This may alter the excretion of drugs that may remain in the body even after their normal washout periods. Hence, this makes it necessary to perform the biodistribution and excretion of the leached elements before using them as a therapeutic strategy.

Further, understanding the fate of the dopants released after oral administration is highly important for optimizing the dose regimens which can be determined from the *in-vivo* pharmacokinetic study (Schwartz and Pateman 2021). It will also help in the context of determining the absorption, tissue distribution, metabolism, and excretion of the released dopants. Moreover, since the kinetic profile of the dopants indirectly determines their residence time in the body, it can also be used to predict the potential adverse effects that they might produce if used for a longer duration (Schwartz and Pateman 2021). Hence, this is the first investigational preclinical study performed to explore the release kinetics of therapeutic ions leached from BG, their pharmacokinetic parameters, biodistribution, and excretion when administered orally in rats. Administration of drugs via the oral route is preferred clinically because of patient compliance and performing oral pharmacokinetic and biodistribution studies will help to elucidate the effects of gastric contents and food on release kinetics.

Therefore, in the present study, the *in-vitro* release kinetics of various dopants from BaBG in SBF and alteration in pH of the solution were accessed using an inductively coupled plasma mass spectrometer (ICP-MS). Further, the changes in plasma concentration of Ca, Ba, and Si after single-dose oral administration of BaBG were studied in rats at various time points and the pharmacokinetic parameters were calculated using the PKSolver software. The distribution of therapeutic dopants from BaBG in various organs and their route of excretion were also investigated in urine and feces. In addition, SEM analysis of the tissue sections of the brain, heart, lungs, liver, kidneys, and spleen of the BaBG-treated rats was performed to analyze the topographical and surface morphological changes in the organs post-BaBG treatment.

3.1. Materials and Methods

3.1.1. Materials

Carboxymethyl cellulose (CMC), paraformaldehyde, glutaraldehyde, and chemicals used to prepare phosphate buffer solution were obtained from SRL, India.

3.1.2. Preparation of Simulated body fluid (SBF)

The *in-vitro* leaching of doped elements from the BG samples was carried out in the SBF solution that was prepared following the procedure mention in section 2.1.3.

3.1.3. *In-vitro* pharmacokinetic study of BaBG

The leaching of dopants from the BG network with respect to time was evaluated in SBF according to the technique suggested by Technical Committee 4 (TC04) of the International Commission on Glass (ICG) (Macon, Kim et al. 2015). The *in vitro* pharmacokinetic study was performed by incubating the glass sample in SBF at a

concentration of 1.5 mg/mL in an airtight polyethylene container to prevent any loss of media; hence avoiding any change in the ratio of glass/SBF. Throughout the experiment, the container was kept in an incubating orbital shaker maintained at 37 °C at 120 rpm. After 0.25, 0.5, 1, 2, 3, 6, 12, 24, 48, 72, 120, and 168 h, 5mL of the solution was removed using a syringe. The solution was then passed through a 0.22 μm Millipore filter and the concentrations of Si, Ca, and Ba were measured with ICP-MS and expressed in ppm.

3.1.4. Animals

The animal experiment was carried out on the adult healthy male albino Wistar rats (200±20 g) that were procured from the Institutional Animal House, IMS- BHU, Varanasi, India. All the experimental rats were acclimatized for 7 days to the laboratory environmental conditions in a controlled temperature of 25 ± 1°C and 45-55 % relative humidity. All throughout the experimental protocol, the experimental animals were kept in a 12:12h light: dark cycle with an *ad libitum* food (Paramount Laboratory Animal feed, Lanka, India) and water supply. During the experimental design, the National Institute of Health Guidelines (publication number 85-23, revised 2013) on animal care experimentation were followed to abridge the number of animals used. The entire experiment was accredited by the Central Animal Ethical Committee of the Indian Institute of Technology (Banaras Hindu University), Varanasi, India (Ref No. IIT(BHU)/IAEC/2022/039).

3.1.5. Experimental design for single dose oral *in-vivo* pharmacokinetic study

The *in-vivo* oral pharmacokinetic study of BaBG was performed in the Wistar rats that were divided into four groups: naïve control, BaBG (1 mg/kg b.w.), BaBG (5 mg/kg

b.w.), and BaBG (10 mg/kg b.w.) (**Figure 3.1**) using the randomization technique. Each group in the study had seven rats. BaBG was suspended in 0.5 % CMC and administered orally to the overnight fasted experimental rats. Subsequently, blood was collected at 1, 24, 48, 72, 120, and 168 h post administration of BaBG from the lateral tail-vein of mildly anaesthetized rats (anaesthetized using diethyl ether) in heparinized centrifuge tubes. Plasma was collected immediately by centrifuging the blood samples at 4000 g (Remi Centrifuge, model number C-24BL, India) for 10 min at 4 °C (Prajapati and Krishnamurthy 2021). The supernatant was decanted and stored at -80 °C until further analysis.

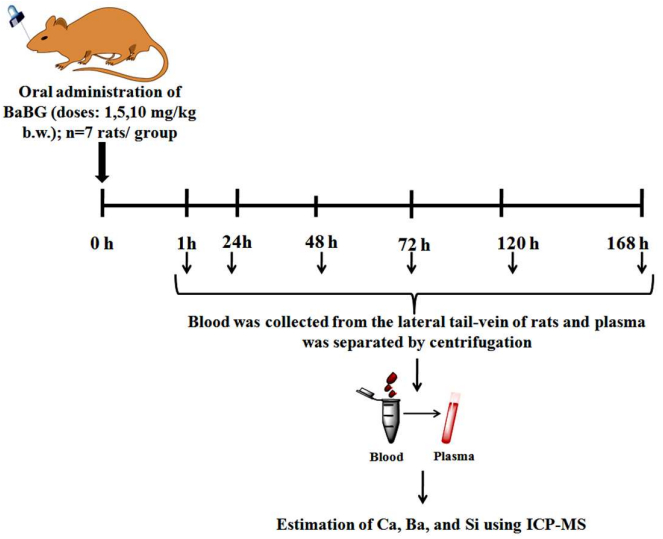

Figure 3.1: Schematic representation of the experimental protocol of the in-vivo single-dose oral pharmacokinetics study of BaBG. The image has been drawn using ChemDraw 15.0.

3.1.6. Pharmacokinetic Analysis

Pharmacokinetic parameters like maximum plasma concentration (C_{max}) and the total time required to reach C_{max} (i.e., T_{max}) of BaBG were obtained from the plasma concentration-time curve (AUC) of BaBG. Similarly, the mean residence time (MRT),

half-life ($t_{1/2}$), volume of distribution (V_z), and clearance (CL) of BaBG were calculated via non-compartmental analysis using the PK Solver software, an 'add-on' for the Microsoft Excel (Zhang, Huo et al. 2010). All the pharmacokinetic parameters are expressed as mean ± SD.

3.1.7. Analysis of Ca, Si, and Ba in urine and feces

To estimate the excretion of Ca, Si, and Ba into urine and feces, the experimental animals during the oral pharmacokinetic study were housed in metabolic cages for sample collection. The urine and fecal samples from each group were collected at the same time points of the pharmacokinetic experimental protocol for evaluating the urinary and fecal excretion of elements (i.e., 0-1, 1-24, 24-48, 48-72, 72-120, 120-168, and 168-192 h). They were weighed immediately, chemically digested, and analyzed by ICP-MS for the presence of Ca, Si, and Ba.

3.1.8. Experimental design for *in-vivo* biodistribution study after single dose oral administration of BaBG

To estimate the distribution of dopants released from BaBG in various organs, the rats were randomly divided into four groups: naïve control, BaBG (1 mg/kg b.w.), BaBG (5 mg/kg b.w.), and BaBG (10 mg/kg b.w.) (n=6 rats/group). The same dose of BaBG that was used during the *in-vivo* pharmacokinetic study was selected and administered orally in the rats (**Figure 3.2**). Post-dosing, at distinct time points (days 1, 3, 5, and 7), the rats of each group were anesthetized using 3 % v/v isoflurane inhalation. Then the animals were sacrificed by cervical dislocation and vital organs like the brain, heart, lungs, liver, kidneys, and spleen were dissected. The organs were weighed and processed for digestion and ICP-MS. The SEM analysis was performed to assess the formation of HA

as well as the surface morphological changes of all the organs collected from the rats of the highest dose group (i.e., 10 mg/kg b.w.) at day 7 post-dosing.

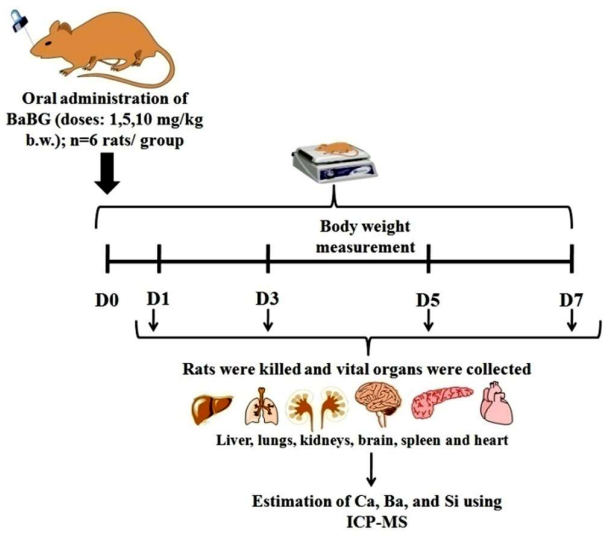

Figure 3.2: Schematic representation of the experimental protocol of the in-vivo biodistribution study after single-dose oral administration of BaBG. The image has been drawn using ChemDraw 15.0

3.1.9. Scanning electron microscopy (SEM) of vital organs

The vital organs like the brain, heart, lungs, kidneys, liver, and spleen collected were fixed in 2.5 % glutaraldehyde solution overnight at 4 °C followed by washing in PBS thrice. Then the tissue samples were dehydrated in a graded series of acetone and dried thoroughly. Subsequently, the dried tissue samples were gold-palladium coated (EMITECH SC 7620) and viewed under the scanning electron microscope (Zeiss EVO LS 10, Carl Zeiss Ltd., Germany) at 10 kV.

3.1.10. Digestion of the biological samples for ICP-MS

Tissue samples of around 300 mg of the vital organs (brain, heart, lungs, kidneys, liver, and spleen) were pre-digested in an acidic condition by incubating the biological samples in a 3 mL mixture of nitric acid and perchloric acid (9:1) for 24 hours. Then

the above mixture was heated at 80 °C for 10 h and again at 140 °C for 30 min. Later on, 2-3 ml of a mixture of nitric acid and perchloric acid was added to the reacting vessel to digest the residue and was further heated at 145 °C till the samples were evaporated to dryness. Finally, 2 % v/v nitric acid solution was added to dissolve the residues and filtered with Whatman filter paper (grade 1, pore size of 11 μm). The filtrate obtained was then diluted to make up the volume up to 5 mL. Similarly, the plasma (300 μL), urine (300 μL), and fecal samples (300 mg) were collected and digested as per the protocol followed for the tissue samples (Dumala, Mangalampalli et al. 2019).

3.1.11. Inductively coupled plasma-mass spectroscopy (ICP-MS)

The concentration of Ca, Si, and Ba present in the digested solutions was performed using ICP-MS which is a single quadrupole type [iCAP-RQ (Thermofisher Scientific, USA)]. The external calibration technique was followed for the quantitative analysis of the samples. The calibration curves for all the analytes were built on 8 different concentrations (0.5-100 ppb), from the limit of detection (LOD) of the corresponding element with the intention that concentrations of all analytes in the samples were within the linear range of the calibration curve. The calibration standards were analyzed at regular intervals during analysis to monitor the instrument drift. Also, ultrapure deionized water blanks were frequently used in the study alongside the samples to check for any loss or cross-contamination. All the measurements were carried out using the full quantitative analysis mode.

3.1.12. Body weight and organ coefficient

During the biodistribution study, the body weight of the animals in each group was weighed before and after BaBG administration. Similarly, at the end of biodistribution experiment for each time-point, the organ (brain, heart, lungs, liver, kidneys, and spleen) weight was recorded and the organ coefficient for every time point was calculated using the following formulae:

$$\text{Organ coefficient} = \left[\frac{\text{Weight of the organ (g)}}{\text{Total body weight (g)}}\right] \text{X}100$$

3.1.13. Statistical analysis

All the data were analyzed statistically by GraphPad Prism Version 8.0 (San Diego, CA, RRID: SCR_002798). The *in-vivo* pharmacokinetic parameters for the released ions were assessed statistically by one-way ANOVA followed by Tukey's multiple comparison tests. The two-way ANOVA followed by the Bonferroni post-hoc test was used to statistically analyze the plasma concentration profile, urinary and fecal excretion, body weight, organ coefficients, and biodistribution of Ca, Ba, and Si. We have considered $p < 0.05$ to be statistically significant in all the analyses, and all the values were presented as mean ± SD.

3.2. Results and discussion

3.2.1. Temporal *in-vitro* release of Ca, Si, and Ba from BaBG in SBF solution

Normally, when BGs react with any physiological fluid like SBF, structural and chemical changes occur and it progresses as a function of time, leading to the accumulation of dissolution products. This series of events ultimately causes alteration in the ionic composition and thus the pH of the reacting fluid. The release of Ca, Si, and

Ba from BaBG post-immersion in SBF solution with respect to time is shown in **Figure 3.3**. After the incubation of BaBG in SBF, the Ca level increased significantly (i.e., 106 ppm) compared to the initial concentration (i.e., 80 ppm) within 30 mins (**Figure 3.3A**). Further, at 1 h, the Ca concentration was 164 ppm and then it increased to 275 ppm at 24 h. According to the theory proposed by Hench et al. (Hench 2006) on the biomineralization of BGs, the increase in the level of Ca is due to the dissolution of the silica framework that leads to rapid leaching of cationic alkali/alkaline earth elements present as oxide network modifiers in the glasses in exchange with H^+ / H_3O^+ from SBF solution. Subsequently, there is a sharp reduction in the Ca concentration from day 3 (72 h) onwards and the Ca level was estimated to be around 148 ppm on day 7 (168 h). This indicates the migration of leached calcium along with phosphate from SBF to the silanol-rich layer on the surface of BaBG. The migration of the elements is considered essential as it leads to nucleation to form calcium phosphate, the precursor of amorphous HA.

Similarly, the concentration of Si was increased and then it gradually decreased as shown in **Figure 3.3B** and reaching maxima at 24 h (i.e., 51 ppm). The composition of SBF as proposed by Kokubo et al. (Kokubo and Takadama 2006) has no Si present in it thus the appearance of Si after immersion of BaBG would have come from the degradation of silica networks in BaBG in a time-dependent manner. However, after 24 h, the level of Si fell steadily until the last day of immersion (i.e., day 7). This reduction in Si may be due to the fact that the leached Si in the SBF solution condenses and repolymerizes to form negatively charged silanol (Hench 2006). Additionally, the amorphous HA layer also starts to deposit on the surface of BaBG, acting as a barrier between the BG surface and SBF; hence, preventing further degradation of the silica

network. Likewise, the leaching profile of the network modifiers in BaBG i.e., Ba is represented in its release curve i.e., **Figure 3.3C** and it exhibited a slow increase within the first few hours, reaching the maximum concentration followed by a reduction in their concentration. The initial phase of release can be attributed to the surface Ba or the isolated Ba species trapped in the vitreous matrix and therefore it does not require extra energy to break the bonds and leach immediately. Further, the later phase of ionic release is due to the incorporated dopants inside the glass matrix. Ba^{2+} has a larger ionic radius (135 p.m.) compared to Ca^{2+} (ionic radius is 100 p.m.) which causes an expanded glass network and decreased oxygen density (Majumdar, Hira et al. 2021). Thus, there is more leaching of the cationic ions from doped BGs than the parent 45S5. Previously, it has also been reported that the incorporation of barium in BaBG has increased the pH of SBF solution compared to the undoped 45S5, thus confirming the dissolution of the silica matrix and release of Ca, Si, and Ba (Majumdar, Hira et al. 2021).

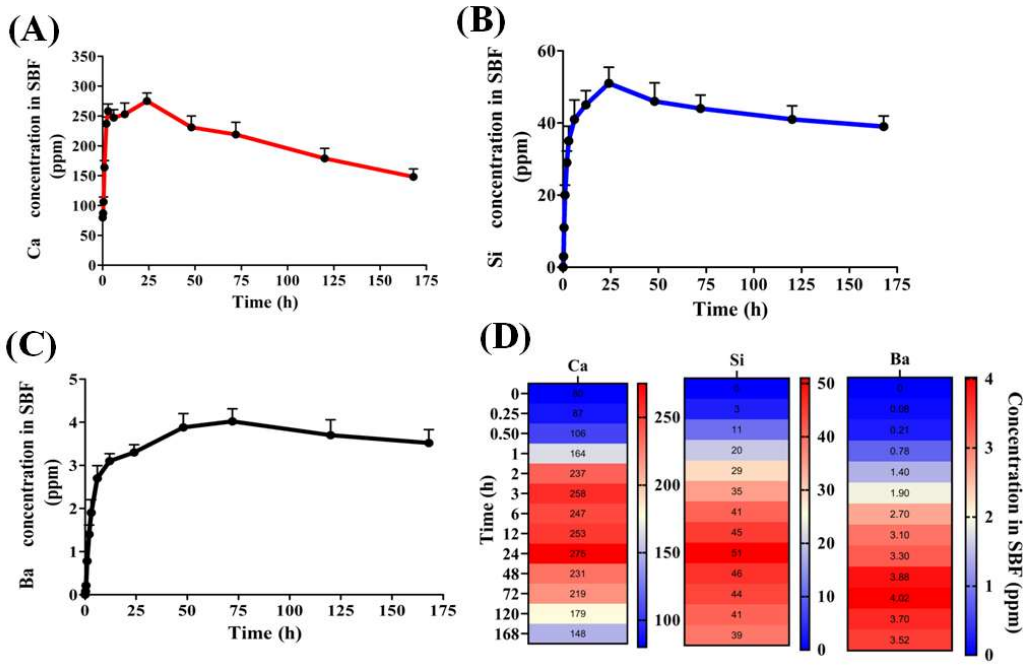

Figure 3.3: The release pattern of Ca (A), Si (B), and Ba (C) in SBF solution at pH 7.4 from BaBG at various time intervals for 7 days using ICP-MS and their representation by heatmap (D).

3.2.2. *In-vivo* oral pharmacokinetic study

3.2.2.1. The plasma concentration of Ca, Ba, and Si released from BaBG in rats during the *in-vivo* pharmacokinetic study

The plasma concentration of the leached Ca, Ba, and Si from BaBG after the oral administration at doses 1, 5, and 10 mg/kg were determined and is represented in **Figure 3.4 (i, ii, and iii)** respectively. The leaching profile of network modifiers is an essential parameter that needs to be evaluated before using inorganic biomaterials therapeutically as they tend to leach dopants that produce several biological effects at the physiological level. However, an increase in their level in the body beyond the physiological level can produce various physiochemical, pharmacokinetic and pharmacodynamic interactions. For instance, antibiotics like tetracycline have been reported to form insoluble metal ion chelation with Ca that reduces its absorption which can affect the bioavailability (Wanner, Walker et al. 1991). Further, the presence of excessive Ca may produce major drug interactions with calcium channel blockers and antiepileptic drugs (Kim, Kim et al. 2022). Therefore, the *in-vivo* release kinetics of the leached dopants from the matrix of BaBG was evaluated. In the present study, the plasma concentration-time curve of Ca and Ba exhibited a dose-dependent increase in their concentration in the plasma from the first hours, reaching maxima at 24 h and then slowly decreasing to the basal level by the end of the experimental protocol (shown in **Figures 3.4i and 3.7ii**). The plasma level of Ba increased maximum to 1.38 ppm at a dose of 10 mg/kg b.w. BaBG (reference level of Ba in the serum of control rats is reported to be around 0.6 ppm (Bligh and Taylor 1963)). Similarly, the calcium level in the plasma of BaBG-treated rats was increased to 55.6 ppm at the highest dose of 10 mg/kg b.w. Statistical analysis by two-way ANOVA revealed significant changes in calcium and barium

concentration in the plasma among the groups ([$F_{(3,144)}$ = 78.84; $p < 0.05$]) and $F_{(3,144)}$ = 164.8; $p < 0.05$]) respectively, time ([$F_{(5,144)}$ = 103.8; $p < 0.05$]) and ([$F_{(5,144)}$ = 244.1; $p < 0.05$]) respectively and, their interaction ([$F_{(15,144)}$ = 15.49; $p < 0.05$]) and([$F_{(15,144)}$ = 53.57; $p < 0.05$]) respectively. The Bonferroni post-hoc analysis revealed a significant increase in the level of both Ca and Ba at 24 h and 48 h at all the doses tested compared to the control rats. The above-observed result suggests that the cations doped in the BG framework were leached in exchange with the H^+ from the acidic gastric fluid in the stomach (Paliwal, Kumar et al. 2018). These released ions are considered to activate a cascade of proteins required for cellular activity over a period of time which may be one of the reasons for the regenerative properties of BaBG in the *in-vitro* model of neurotrauma (Majumdar, Hira et al. 2021). Further, every element in our body has a physiological and pharmacological limit and an uncontrolled and unchecked release of therapeutic dopants from BGs may lead to adverse effects. In this case, the increase in the level of Ba is within the safety limits and is also considered non-toxic as per the acute and sub-acute oral toxicity study performed in rats (Majumdar and Krishnamurthy 2022).

The network modifiers i.e., Ca and Ba, after their uphill increment till 24h showed a gradual dip in their concentration in the plasma. The gradual decrease in calcium concentration in plasma after 24 h maybe due to its accumulation over the silanol-rich layer form an amorphous HA layer (as observed in XRD and FTIR during *in vitro* study). Additionally, since Ca is an endogenous element in the body, therefore; an increase in its level is re-established naturally to the basal level through various physiological pathways. There are many calcium homeostasis-maintaining mechanisms that include its influx and efflux by the activation of various calcium transporter/

channels, hormonal regulation through calcitonin, parathyroid hormone, and Vitamin D3, and also by deposition in various organs and bones (Matikainen, Pekkarinen et al. 2021). Similarly, the decrease in the level of Ba after 24 h may be because it is rapidly excreted out of the body mainly through the fecal matter as observed during the excretion studies (**Table 3.6**). Moreover, there was a dose-dependent increase in the clearance (CL) of Ba from the plasma and at a dose 10 mg/kg, CL increased by around 3-fold compared to 1 mg/kg (**Table 3.2**). Ba accumulated mainly in the metabolizing and excretory organs like the liver and kidneys (**Table 3.7**). Ba has also been reported to get deposited mostly in the hard osseous tissues like the skeleton and teeth and also in fats (Kravchenko, Darrah et al. 2014, Kovrlija, Locs et al. 2021), which may have caused the decrease in Ba plasma level after the observed C_{max} at 24 h (**Table 3.2**).

Similarly, after the oral administration of BaBG, there was a statistically significant increase in the level of Si in plasma at all doses compared to the control rats followed by a gradual decrease (as shown in **Figure 3.4iii**). The reference level of the reported Si level in control rats is 3 ppm (Du, Chen et al. 2019). The initial phase of increased Si in the plasma of treated rats may be due to the dissolution of the silicate networks of BaBG in the presence of physiological fluid (Hench 2006). Then the leached Si is absorbed into the systemic circulation through the gastrointestinal epithelium. However, by the end of day 3, the elevated level of Si was found to be statistically insignificant and at the end of day 7, it was similar to the basal level of Si present in the plasma of control rodents. This reduction in the level of Si may be due to the biodistribution of Si to various tissue compartments. Meanwhile, after the oral administration of BaBG, Si was remarkably higher in the spleen and liver which may be due to the uptake by the reticuloendothelial system (RES) and kuffer cells

respectively (as represented in **Table 3.7**) as similarly reported by Lee et al. (Lee, Kim et al. 2014).

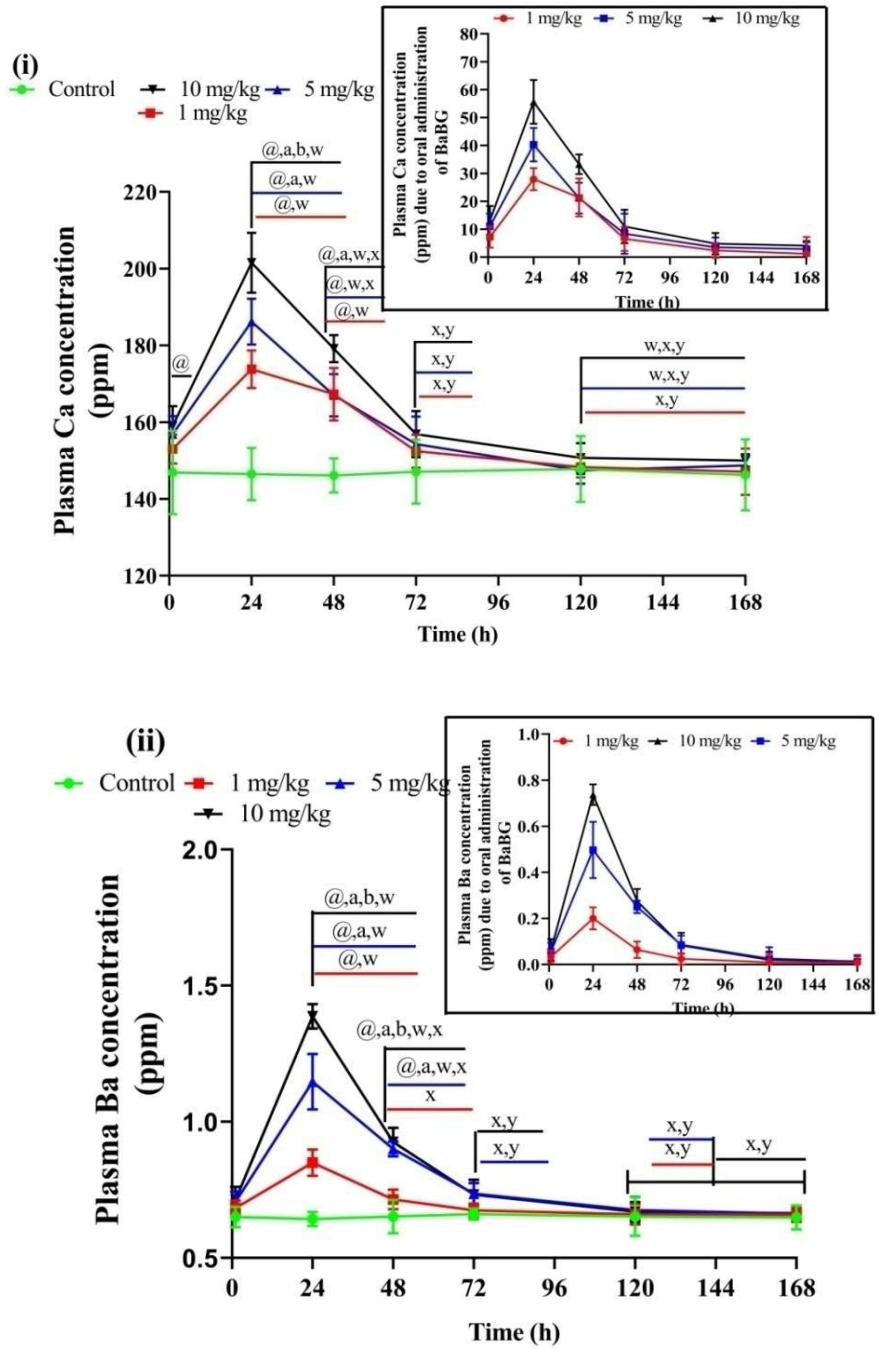

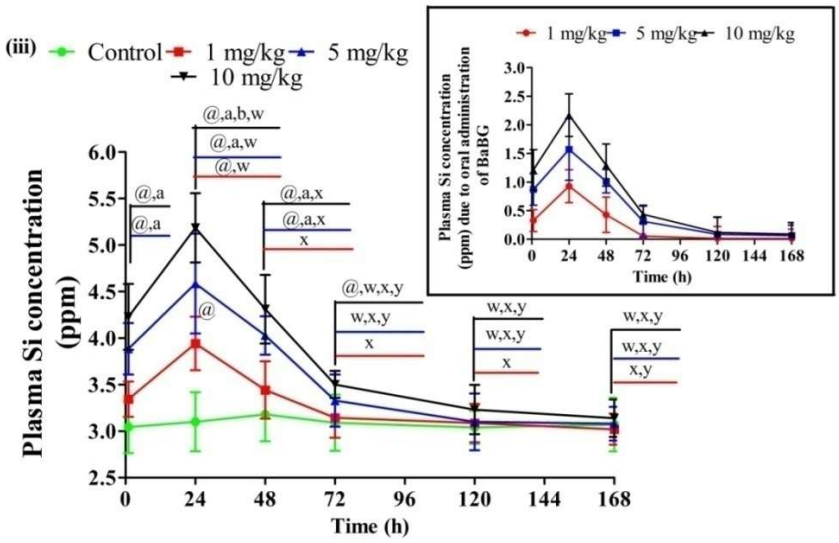

Figure 3.4: Plasma concentration profile of Ca (i), Ba (ii), and Si (iii) released from BaBG administered orally. All values are in mean ± SD (n=7 rats/ group).). $^{@}p<0.05$, $^{a}p<0.05$, and $^{b}p<0.05$ compared to control, dose 1mg/kg and 5 mg/kg of BaBG respectively. $^{w}p<0.05$, $^{x}p<0.05$, and $^{y}p<0.05$compared to 1, 24, 48 h respectively (Two-way ANOVA followed by Bonferroni post-hoc test).

3.2.2.2. *In-vivo* oral pharmacokinetic profile of Ca, Ba, and Si released from BaBG

The addition of network modifiers like CaO and BaO into the silica network of BGs tends to change the framework of BaBG which may alter the dissolution kinetics and hence the pharmacokinetic parameters. Therefore, the pharmacokinetic parameters of the released therapeutic ions (Ca, Ba, and Si) from BaBG after its oral administration were estimated and are reported in **Tables 3.1, 3.2, and 3.3** respectively. The maximum concentration of Ca observed in the plasma (C_{max}) after the oral administration at doses 1, 5, and 10 mg/kg was 27.93 ± 3.02, 40.28 ± 5.19, and 55.62 ± 4.48 ppm respectively and statistical analysis by one-way ANOVA followed by Tukey's post-hoc test revealed significant differences between them. However, the time taken to reach C_{max} (i.e., T_{max}) was the same for all the doses and was observed at 24 h. Moreover, the time taken for the concentration of Ca in plasma to reduce by 50% (i.e., $t_{1/2}$) was found to be 39.27 ± 3.72, 37.08 ± 2.99, and 36.85 ± 3.08 h for 1, 5, and 10 mg/kg respectively and was

statistically insignificant ($p > 0.05$). We also observed that the volume of distribution (V_z) and mean residence time (MRT) for Ca was increased in a dose-dependent manner (as shown in **Table 3.1**). Since $t_{1/2}$ is a composite pharmacokinetic parameter which is determined by V_z, hence, it can be ascertained that Ca in the blood circulation is biodistributed and is more concentrated in tissue compartments than in the vascular compartment of the body after its release from BaBG which corroborated the biodistribution study results (**Table 3.7**). Further, with an increase in dose, Ca leached from BaBG exhibited longer MRT. This may be due to the reason that around 98 % of filtered Ca gets reabsorbed by the renal tubules of kidneys (Blaine, Chonchol et al. 2015) by passive diffusion or solvent drag under normal physiological conditions. Additionally, the increased Ca are also removed from the blood circulation by binding to serum albumin non-covalently (Blaine, Chonchol et al. 2015); hence, longer MRT with the increase in the dose of BaBG.

Similarly, after the oral administration of BaBG, Ba ions are leached from the BG framework and enter the systemic circulation by absorption through the biological membrane. The course of movement of the leached dopants throughout the body before their excretion is essential to elucidate the extent of therapeutic effects as well as the toxic effects they might produce. Hence, the pharmacokinetic parameters of Ba released from BaBG were determined and are represented in **Table 3.2**. In the present study, after the leaching of Ba in the GIT, they are absorbed which caused a significant increase in the C_{max} of Ba in a dose-dependent manner similar to Ca in plasma. The T_{max} was observed at 24 h for all the doses. The C_{max} increased to more than double at a dose of 5 mg/kg b.w. (i.e. 0.49 ± 0.0488 ppm) compared to 1 mg/kg (0.22 ± 0.0189 ppm). Similarly, at dose 10 mg/kg, C_{max} increased significantly to 1.38 ppm compared to both

doses (1 and 5 mg/kg b.w.; $p<0.05$). The increased C_{max} for Ba in plasma with dose sheds light on the fact that the leached barium was absorbed through the gastrointestinal epithelium and has reached the blood circulation. However, on the contrary to Ca, the $t_{1/2}$ and MRT for Ba decreased in a dose-dependent manner and the specific reason explaining this trend remains unclear. The biodistribution pattern of the divalent Ba after their absorption from the GIT may help to explain this unusual trend. From the above results, it can also be presumed that after reaching the highest plasma concentration at 24 h, the physiological hemostasis set-point for barium is broken. As a result, irrespective of increased C_{max} with an increase in dose, there is a decrease in $t_{1/2}$ and MRT for doses 5 and 10 mg/kg compared to the lowest dose (i.e., 1 mg/kg b.w.). In general, the body tries to maintain homeostasis by distributing it to other body compartments or by excreting it. It has been observed that biologically non-essential elements like Ba have the tendency to get rapidly deposited mainly in less perfused mineralized organs like the skeleton systems (Bligh and Taylor 1963, Panahifar, Chapman et al. 2019). Ba having larger ionic radii than Ca gets more readily adsorbed in the form of colloidal particles on the surface of bones that help in the calcification process. Additionally, Ba was rapidly excreted in the feces since the body has the tendency to reduce the load of non-essential elements from the body as evidenced by the increased clearance (as represented in **Table 3.5**) with the increased dose which was statistically significant ($p<0.05$). Therefore, from the above-mentioned results, we can say that the increased level of Ba in blood circulation is normalized by physiological homeostatic pathways including biodistribution and excretion.

Further, in the case of Si, the C_{max} increased with dose and was found to be 0.93 ± 0.073, 1.57 ± 0.184, and 2.18 ± 0.206 ppm for 1, 5, and 10 mg/kg b.w. respectively and the

T_{max} was observed at 24 h for all the doses (as shown in **Table 3.3**). Furthermore, another important pharmacokinetic parameter is Vz which was also found to be augmented by approx. 2.8 and 4.2-fold at doses 5 and 10 mg/kg compared to 1mg/kg. Higher Vz indicates that the absorbed Si in the vascular compartment has a high tendency to escape the blood circulation and enter the extravascular compartments as observed during the biodistribution study (**Table 3.7**). Similarly, the MRT of Si in the body for doses 5 and 10 mg/kg was significantly higher compared to 1 mg/kg ($p<0.05$) which can be due to enhanced distribution in various tissues. Studies have reported that Si accumulation in various organs mainly the liver and spleen was observed for 3 days in rats (Lee, Kim et al. 2014). As per the previous study, there was no accumulated organ toxicity of BaBG in rats when administered orally at a dose up to 1000 mg/kg b.w. (Majumdar and Krishnamurthy 2022).

Table 3.1: Pharmacokinetic parameters for Ca released after single-dose oral administration of BaBG

Pharmacokinetic parameters	1 mg/kg BaBG	5 mg/kg BaBG	10 mg/kg BaBG
Half life ($t_{1/2}$) (h)	39.27± 3.72	37.08± 2.99	36.85± 3.08
T_{max}(h)	24	24	24
C_{max}(ppm)	27.93± 3.02	40.28± 5.19[a]	55.62± 4.48[a,b]
AUC $_{0\text{-}t}$ (ppm.h)	1636.01± 32.98	2127.17± 27.38[a]	2989.02± 40.96[a,b]
Vz (mg/kg)/(ppm)	0.0332± 0.002	0.1171± 0.003[a]	0.1657±0.021[a,b]
CL (mg/kg)/(ppm)/h	0.00058± 0.000071	0.00219± 0.00025[a]	0.00311± 0.00039[a,b]
MRT (h)	53.72 ± 5.34	59.12± 4.90	59.59± 4.16

All data are expressed as mean ± SD (n = 7 male rats/ group). [a]$p<0.05$ and [b]$p < 0.05$ compared to 1 and 5 mg/kg b.w. respectively. (One-way ANOVA followed by Tukey's multiple comparison post-hoc tests)

Table 3.2: Pharmacokinetic parameters for Ba released after single-dose oral administration of BaBG

Pharmacokinetic parameters	1 mg/kg BaBG	5 mg/kg BaBG	10 mg/kg BaBG
Half life ($t_{1/2}$) (h)	31.62± 2.88	26.47 ± 2.05[a]	24.72 ± 2.71[a]
T_{max}(h)	24	24	24
C_{max}(ppm)	0.22± 0.0189	0.49 ± 0.0488[a]	0.73±0.064[a,b]
AUC $_{0\text{-}t}$ (ppm.h)	8.804± 0.65	23.67 ± 1.93[a]	28.97 ±2.52[a,b]
Vz (mg/kg)/(ppm)	4.961± 0.37	7.904 ± 0.84[a]	12.101 ±0.99[a,b]
CL(mg/kg)/(ppm)/h	0.109± 0.0078	0.207 ± 0.0154[a]	0.339 ±0.0316[a,b]
MRT (h)	48.26± 3.91	46.79 ± 4.05	41.51 ± 3.98[a]

All data are expressed as mean ± SD (n = 7 male rats/ group).[a]$p<0.05$ and [b]$p < 0.05$ compared to 1 and 5 mg/kg b.w. respectively. (One-way ANOVA followed by Tukey's multiple comparison post-hoc tests)

Table 3.3: Pharmacokinetic parameters for Si released after single-dose oral administration of BaBG

Pharmacokinetic parameters	1 mg/kg BaBG	5 mg/kg BaBG	10 mg/kg BaBG
Half life ($t_{1/2}$) (h)	22.31 ± 2.51	29.24 ±1.96[a]	29.95 ± 3.04[a]
T_{max}(h)	24	24	24
C_{max}(ppm)	0.93 ± 0.073	1.57 ± 0.184[a]	2.18 ±0.206[a,b]
AUC $_{0\text{-}t}$ (ppm.h)	39.24 ± 4.26	88.73 ± 7.21[a]	120.32 ±9.13[a,b]
Vz (mg/kg)/(ppm)	0.812 ± 0.071	2.305 ±0.181[a]	3.432 ±0.244[a,b]
CL(mg/kg)/(ppm)/h	0.0252 ± 0.0019	0.054 ± 0.0043[a]	0.081 ±0.0075[a,b]
MRT (h)	35.33 ±3.04	46.13 ± 4.13[a]	47.17 ± 3.86[a]

All data are expressed as mean ± SD (n = 7 male rats/ group).[a]$p<0.05$ and [b]$p < 0.05$ compared to 1 and 5 mg/kg b.w. respectively. (One-way ANOVA followed by Tukey's multiple comparison post-hoc tests)

3.2.3. Urinary and fecal excretion

The inorganic biomaterials are considered biologically safe and can be translated clinically only if they have a controlled rate of elimination and metabolism. Therefore, the excretion kinetics of Ca, Ba, and Si released from BaBG after the oral administration were evaluated and are represented in **Tables 3.4, 3.5, and 3.6** respectively. The clearance of any inorganic compound from the body follows two

major eliminating routes i.e., hepatobiliary and fecal excretion and urinary excretion, hence, we temporally measured the level of Ca, Ba, and Si in urine and feces. It was observed that the cumulative amount of Ca excreted in urine and feces increased with the dose of BaBG (**Table 3.4**). Statistical analysis by two-way ANOVA exhibited significant changes in Ca level in the urine and feces among the groups ([$F_{(3,168)}$ = 271.5; $p < 0.05$] and $F_{(3,168)}$ = 162.5; $p < 0.05$] respectively), time ([$F_{(6,168)}$ = 1434; $p < 0.05$] and [$F_{(6,168)}$ = 2031; $p < 0.05$] respectively) and, their interaction ([$F_{(18,168)}$ = 7.664; $p < 0.05$] and [$F_{(18,168)}$ = 5.606; $p < 0.05$] respectively). The post-hoc analysis revealed a significant increase in the level of Ca in the urine and feces from 24 h onwards at doses 5 and 10 mg/kg compared to the control group. The above-observed results have been similar to the previous report where calcium is excreted mainly through urine and feces to maintain the body's homeostasis (Ross, Taylor et al. 2012). However, after the glomerular filtration of Ca by kidneys, 80% of the filtered Ca is reabsorbed via passive diffusion or solvent drag in the proximal tubule (Ross, Taylor et al. 2012). It is also noteworthy that, in our study, the cumulative excretion of Ca was more in feces than in urine. We speculate that BaBG tends to get adsorbed into the mucous layer of the stomach after oral administration (**Figure 3.7**). This protective layer (mucus) has the tendency to continuously renew itself and is removed from the site, travels to the lower GIT and is excreted in feces. Therefore, Ca released into the lower GIT from the trapped BaBG in mucus has the lesser opportunity to get absorbed, leading to increased Ca levels in feces.

Similarly, in the excretion kinetic study of Ba, there was an increase in the level of Ba in both the urine and feces dose-dependently like Ca (shown in **Table 3.5)**. Normally, Ba released from BaBG are absorbed into the blood through the biological membrane

of GIT and then the body tries to restore homeostasis by distributing it to the bones and excretion through urine and feces (Moffett, Smith-Simon et al. 2007, Kravchenko, Darrah et al. 2014). Likewise, in our study, we observed that the plasma level of Ba after the oral administration of BaBG followed a downhill fall after the observed T_{max} at 24 h (**Figure 3.4ii**). The fall in the level of Ba may be due to increased clearance dose-dependently (**Table 3.2**) as Ba is a non-essential element and the body tries to eliminate it to restore homeostasis. We also observed that the fecal excretion of Ba exceeded the urinary excretion. In support of our observation, a study published indicated feces to be the primary route of excretion of Ba in rats that were exposed to barium chloride in their diet (Stoewsand, Anderson et al. 1988). Similarly, in the biodistribution study, the Ba level was higher in the liver compared to the kidneys (**Table 3.7**). The deposited Ba in the liver is most likely to get secreted in bile and thereby excreted out in feces.

The elimination kinetics of Si leached from BaBG after the single dose oral administration is represented in **Table 3.6** and statistical analysis by two-way ANOVA followed by post-hoc test exhibited significant elevation in the level of Si in urine and feces compared to the control rats. The detection of Si in urine implies that the kidneys are one of the excreting organs and even in the biodistribution study of BaBG, Si was detected more in the kidneys and liver compared to other organs (**Table 3.7**). Normally, Si that enters the systemic circulation after absorption through the intestinal mucosa follows the renal route of excretion without affecting the microstructure of the kidneys (Majumdar and Krishnamurthy 2022).

Table 3.4: Urinary and fecal excretion of Ca post-oral administration of BaBG in rats

Doses of BaBG (mg/kg b.w.)	Cumulative amount excreted in urine (ppm)						
	0-1h	1-24 h	24-48 h	48-72 h	72-120 h	120-168 h	168-192h
Control	20.48±3.78	38.88±3.26	56.10±4.91	77.49 ±5.15	105.54 ±6.84	120.37 ±9.79	139.39 ±3.27
1	22.19±2.15	50.26±4.26	75.65±8.35$^{@}$	98.76 ±7.84$^{@}$	118.69 ±4.12$^{@}$	138.90±7.23$^{@}$	154.94±9.91$^{@}$
5	25.44±2.03	59.57±7.07$^{@}$	89.78 ±6.07$^{@,a}$	112.26±10.52$^{@,a}$	129.70±10.83$^{@,a}$	147.78±3.68$^{@,a}$	167.39±5.38$^{@,a}$
10	26.32±4.11	66.34±5.73$^{@,a}$	101.14±8.72$^{@,a,b}$	127.47±5.37$^{@,a,b}$	157.58±13.42$^{@,a,b}$	167.61±7.71$^{@,a,b}$	181.87±6.22$^{@,a,b}$
	Cumulative amount excreted in feces (ppm)						
Control	35.82±1.45	74.13±8.82	114.14±13.20	146.19±8.81	181.76±14.49	220.47±15.35	254.70±18.02
1	33.03±3.89	79.05±9.16	121.32±10.26	152.41±6.78	192.63±5.24	235.07±6.16	275.45±12.52$^{@}$
5	40.16±4.19	93.67±7.90$^{@}$	144.71±11.33$^{@,a}$	175.38±10.04$^{@,a}$	201.72±10.72$^{@,a}$	251.57±10.73$^{@,a}$	292.84±9.75$^{@,a}$
10	37.54±5.28	102.71±12.23$^{@,a}$	161.82±4.04$^{@,a,b}$	192.27±5.27$^{@,a,b}$	235.25±8.06$^{@,a,b}$	279.73±11.47$^{@,a,b}$	310.80±17.79$^{@,a,b}$

Data are expressed as mean ± SD (n = 7 male rats/group). $^{@}p<0.05$, $^{a}p<0.05$ and $^{b}p<0.05$ compared to control, 1, and 5 mg/kg b.w. respectively (Two-way ANOVA followed by Bonferroni post-hoc test).

Table 3.5: Urinary and fecal excretion of Ba post-oral administration of BaBG in rats

Doses of BaBG (mg/kg b.w.)	Cumulative amount excreted in urine (ppm)						
	0-1h	1-24 h	24-48 h	48-72 h	72-120 h	120-168 h	168-192h
Control	0.41 ±0.083	0.78 ±0.052	1.08 ±0.28	1.35 ±0.34	1.70 ±0.20	2.12 ±0.36	2.43 ±0.42
1	0.39 ±0.051	0.79 ±0.094	1.41 ±0.35	1.89±0.19$^{@}$	2.15 ±0.37$^{@}$	2.42 ±0.28	2.80 ±0.3
5	0.43 ±0.037	0.96 ±0.046	1.45 ±0.18	1.92±0.22$^{@}$	2.21 ±0.41$^{@}$	2.69 ±0.23$^{@}$	3.11±0.28$^{@,a}$
10	0.48 ±0.066	1.12 ±0.18	1.70 ±0.28$^{@}$	2.20 ±0.39$^{@}$	2.67 ±0.18$^{@,a,b}$	3.15 ±0.41$^{@,a,b}$	3.61 ±0.42$^{@,a,b}$
	Cumulative amount excreted in feces (ppm)						
Control	0.38 ±0.016	0.68±0.092	1.08 ±0.15	1.48 ±0.17	1.83 ±0.37	2.24 ±0.14	2.68 ±0.28
1	0.40 ±0.025	0.84 ±0.056	1.42 ±0.21	1.91 ±0.27$^{@}$	2.33 ±0.18$^{@}$	2.72 ±0.35$^{@}$	3.06 ±0.31
5	0.42 ±0.073	0.89 ±0.12	1.61±0.17$^{@}$	2.03 ±0.29$^{@}$	2.61 ±0.39$^{@}$	3.03 ±0.44$^{@}$	3.49 ±0.46$^{@,a}$
10	0.37 ±0.028	1.12±0.19	1.98±0.24$^{@,a,b}$	2.71 ±0.35$^{@,a,b}$	3.08±0.42$^{@,a,b}$	3.85 ±0.41$^{@,a,b}$	4.25 ±0.57$^{@,a,b}$

Data are expressed as mean ± SD (n = 7 male rats/group).$^{@}p<0.05$, $^{a}p<0.05$ and $^{b}p<0.05$ compared to control, 1, and 5 mg/kg b.w. respectively (Two-way ANOVA followed by Bonferroni post-hoc test).

Table 3.6: Urinary and fecal excretion of Si post-oral administration of BaBG in rats

Doses of BaBG (mg/kg b.w.)	Cumulative amount excreted in urine (ppm)						
	0-1h	**1-24 h**	**24-48 h**	**48-72 h**	**72-120 h**	**120-168 h**	**168-192h**
Control	1.03±0.12	2.11±0.27	2.64±0.34	3.17±0.18	3.75±0.27	4.14±0.28	4.73±0.32
1	1.65±0.19	2.36±0.16	3.09±0.32	3.68±0.29$^{@}$	4.22±0.21$^{@}$	4.81±0.41$^{@}$	5.32±0.28$^{@}$
5	1.51±0.11	2.62±0.23$^{@}$	3.19±0.39$^{@}$	3.89±0.24$^{@}$	4.38±0.13$^{@}$	5.08±0.51$^{@}$	5.75±0.41$^{@}$
10	1.72±0.17$^{@}$	2.83±0.24$^{@,a}$	3.67±0.40$^{@,a,b}$	4.17±0.38$^{@,a}$	4.82±0.36$^{@,a}$	5.69±0.33$^{@,a,b}$	6.37±0.74$^{@,a,b}$
	Cumulative amount excreted in feces (ppm)						
Control	0.72±0.17	1.72±0.27	2.72±0.35	3.78±0.31	4.76±0.64	5.89±0.66	6.62±0.85
1	1.01±0.23	2.89±0.15$^{@}$	4.15±0.39$^{@}$	5.21±0.27$^{@}$	6.13±0.46$^{@}$	7.09±0.37$^{@}$	7.74±0.43$^{@}$
5	0.94±0.084	3.19±0.28$^{@}$	4.39±0.45$^{@}$	5.84±0.53$^{@,a}$	7.01±0.32$^{@,a}$	7.81±0.40$^{@,a}$	8.88±0.74$^{@,a}$
10	0.88±0.26	3.66±0.13$^{@,a}$	5.27±0.35$^{@,a,b}$	7.62±0.49$^{@,a,b}$	8.85±0.61$^{@,a,b}$	9.39±0.54$^{@,a,b}$	10.03±0.52$^{@,a,b}$

Data are expressed as mean ± SD (n = 7 male rats/group).$^{@}p<0.05$,$^{a}p<0.05$, and $^{b}p<0.05$ compared to control, 1mg/kg, and 5 mg/kg b.w. dose of BaBG respectively (Two-way ANOVA followed by Bonferroni post-hoc test).

3.2.4. Changes in body weight and organ coefficient after oral administration of BaBG

In the temporal biodistribution study of BaBG at different doses, the body weight and the organ coefficient of the treated rats were measured as they are the essential parameters to ascertain the normal physiological functioning of the internal organs. Therefore, the body weight of the rats treated with BaBG at doses 1, 5, and 10 mg/kg were measured (data not shown). Statistical analysis by two-way ANOVA showed no significant differences between the body weights of rats in every group ($p > 0.05$). Moreover, the organ coefficients of various vital organs like the brain, heart, lungs, liver, kidneys, and spleen were also statistically insignificant ($p > 0.05$) compared to the control group. This confirms that the doses selected for the pharmacokinetic and biodistribution study were safer and these findings are in agreement with our previous report (Majumdar and Krishnamurthy 2022) where BaBG was found to be non-toxic as per the OECD acute and sub-acute toxicity study performed on rats.

3.2.5. *In-vivo* biodistribution of Ca, Ba, and Si in vital organs and their scanning electron microscopical analysis

When any inorganic-based biomaterials are designed to be used systemically for therapeutic purposes and have a longer MRT, their organ accumulation and biodistribution in the body is an essential parameter that needs to be studied. This will help in optimizing the dosage regimen including the route of administration, dose, dosing interval and the duration of treatment. Biodistribution studies also assist in elucidating the potential organ toxicity or cumulative toxicity that the test compounds might produce. During the *in-vivo* pharmacokinetic study, the circulation half-life of

Ca, Ba, and Si was found to be 36.85 ± 3.08, 24.71 ± 2.71, and 29.95 ± 3.04 h respectively (**Table 3.1, 3.2, and 3.3**) at the highest dose tested, thus demonstrating a longer circulation in the body. Hence, the biodistribution of BaBG after oral administration was evaluated in vital organs. As shown in **Table 3.7** and **Figure 3.6**, there was a dose-dependent increase in the level of Ca, Ba, and Si in the vital organs (brain, liver, heart, kidneys, lungs, and spleen). At day 1 (D 1) post-administration of BaBG, there was a statistically significant level of calcium detected in the liver, kidneys, and spleen at a dose of 5 mg/kg compared to the control group. However, at the highest dose, a statistically significant level of Ca was detected in all the organs compared to the control rats ($p < 0.05$). As time progressed, at D 3, the amount detected in all the organs increased further and at 10 mg/kg, the increase was almost 1.2-fold compared to D 1. One possible reason may be that after the absorption of leached Ca from BaBG into the systemic circulation, the body tries to maintain homeostasis. There are various physiological calcium stores in the body where the surplus of calcium is stored (CHENG, Wei et al. 2006, Patel and Docampo 2010). Additionally, the rapid increase in Ca level was drastically reduced through urine as a statistically significant amount of Ca was detected in the kidneys (**Table 3.7**). In the SEM of the kidney tissue sections of BaBG-treated rats (10 mg/kg), there was the presence of HA (as represented in **Figure 3.6iii**). HA are biocompatible endogenous substances which are biodegradable and their deposition did not affect the microarchitecture or physiological functioning of kidneys during sub-acute toxicity study performed in rats (Majumdar and Krishnamurthy 2022). Furthermore, we also observed a higher percentage of Ca accumulation in the spleen compared to other organs from D 1 along with the deposition of HA (**Figure 3.6ii**). The reason may be that the body has normal physiological

phenomena to eliminate foreign particles that enter the systemic circulation by phagocytosis into the spleen through the splenic artery. So, either BaBG of smaller size would have been absorbed into the blood from GIT or HA formed *in situ* in the stomach (as observed in the SEM of the stomach tissue in **Figure 3.5**) may have migrated to the splenic tissue. Similarly, the liver is also involved in the endocytosis of foreign entities (BaBG) via the resident mononuclear macrophages of the RES that are abundantly present (Bhandari, Larsen et al. 2021). Subsequently, from D 5 onwards, the Ca level followed a downhill pattern and after day 7, we did not find statistically elevated levels of Ca in any of the major organs.

After the dissolution of the glass network, there is simultaneous leaching of Si and Ba in the *in-vitro* dissolution study in SBF (**Figure 3.3**). Similarly, in the *in-vivo* study, there was early detection of these elements in the liver and spleen on D 1 (**Table 3.7**). Their presence may be due to the opsonization of glass particles by the sinusoidal endothelial cells and Kupffer cells of the liver and phagocytes of the spleen, the major organs for removing the circulating exogenous entities. Statistical analysis by two-way ANOVA exhibited significant elevation in the level of Siand Ba at doses 5 and 10 mg/kg compared to the control group at D 1. Ba increased to 2.53 and 1.28 fold in the spleen and liver respectively at the highest dose while Si was elevated by approx. 1.5 fold in these eliminating organs. A previous study based on the silica-based nanoparticle showed that they were absorbed from the intestin eepithelium and are reportedly redistributed mainly in the liver and spleen (Fu, Liu et al. 2013). Normally, after the oral administration of any inorganic biomaterials, they are absorbed into the portal vein from the intestine and reache the liver. This could be one possible reason for the presence of HA in the liver (as represented in **Figure 3.6i**). Similarly, Ba and Si content

were also elevated significatly in the kidneys from D 1 after oral exposure compared to the control group. For Si, there was a more than 2-fold increase in its level in the kidneys. On the other hand, Ba and Si were in relatively lower concentration in the brain and lungs (**Table 3.7**). The Ba and Si concentrations reached the peak at D 3 like Ca in a dose-dependent manner followed by a reduction and levelling off to the basal level. It reflects that there is a dose-dependent elevation in the concentration of elements leached from BaBG. Therefore, dose selection should be done cautiously when employing BG for oral or systemic administration during therapeutic intervention.

Table 3.7: Tissue concentration of Ca, Ba, and Si in the brain, heart, lungs, liver, kidneys, and spleen after single-dose oral administration of BaBG at doses 1, 5, and 10 mg/kg b.w. at days 1, 3, 5, and 7

(i)	Concentration of Ca (ppm) in Brain				Concentration of Ba (ppm) in Brain			
	D1	D3	D5	D7	D1	D3	D5	D7
Control	9.61±1.78	10.23±0.93	10.17±1.22	9.74±0.90	0.0067±0.0014	0.0062±0.00084	0.0060±0.0011	0.0068±0.0007
BaBG-1	10.28±0.85	11.89±1.43	9.92±0.75^{y}	9.87±1.07^{y}	0.0063±0.0013	0.0072±0.0006	0.0068±0.0017	0.0066±0.0005
BaBG-5	10.94±1.71	12.27±1.02$^{@}$	10.01±1.46^{y}	9.63±1.21^{y}	0.0067±0.0007	0.0078±0.0012$^{@}$	0.0070±0.0004	0.0065±0.0007
BaBG-10	11.53±2.03$^{@}$	12.92±0.96$^{@}$	10.38±0.37^{y}	10.11±0.89^{y}	0.0069±0.0011	0.0081±0.0003$^{@}$	0.0071±0.0012	0.0062±0.0016^{y}
(ii)	Concentration of Ca (ppm) in Lungs				Concentration of Ba (ppm) in Lungs			
	D1	D3	D5	D7	D1	D3	D5	D7
Control	157.62±14.12	160.02±13.98	151.91±10.12	159.21±16.04	0.045±0.0068	0.050±0.0044	0.049±0.0086	0.044±0.0071
BaBG-1	163.07±12.17	171.11±7.77	160.48±9.83	158.96±7.51	0.056±0.0061	0.063±0.0059$^{@}$	0.050±0.0028^{y}	0.047±0.0067^{y}
BaBG-5	170.50±6.91	180.56±9.09$^{@}$	161.23±17.15^{y}	163.60±10.89	0.061±0.0078$^{@}$	0.072±0.0034$^{@}$	0.058±0.0060^{y}	0.049±0.0054^{y}
BaBG-10	177.68±15.98$^{@}$	191.78±10.13$^{@,a}$	167.41±8.03^{y}	160.70±13.68^{y}	0.070±0.0044$^{@,a}$	0.083±0.0061$^{@,a,x}$	0.061±0.0081^{y}	0.053±0.023^{x,y}
(iii)	Concentration of Ca (ppm) in Heart				Concentration of Ba (ppm) in Heart			
	D1	D3	D5	D7	D1	D3	D5	D7
Control	81.03±10.93	84.35±7.01	89.16±8.80	80.99±11.27	0.014±0.0034	0.014±0.0047	0.012±0.0024	0.015±0.0061
BaBG-1	89.02±6.59	96.19±10.11	80.22±4.48^{y}	84.41±5.87	0.019±0.0026	0.021±0.0016	0.015±0.0010	0.013±0.0057^{y}
BaBG-5	94.48±12.03	100.39±9.87$^{@}$	90.78±7.42	86.29±6.26^{y}	0.023±0.0067$^{@}$	0.034±0.0073$^{@,a,x}$	0.019±0.0035^{y}	0.015±0.0072^{x,y}
BaBG-10	101.66±8.13$^{@,a}$	113.01±13.17$^{@,a}$	96.97±10.39$^{@,y}$	82.72±9.94^{x,y,z}	0.030±0.0051$^{@,a}$	0.041±0.0039$^{@,a,x}$	0.021±0.0060$^{@,x,y}$	0.017±0.0028^{x,y}
(iv)	Concentration of Ca (ppm) in Liver				Concentration of Ba (ppm) in Liver			
	D1	D3	D5	D7	D1	D3	D5	D7
Control	9.36±1.21	9.19±1.09	9.40±0.72	9.03±0.83	0.072±0.0081	0.078±0.0093	0.074±0.0055	0.080±0.0123
BaBG-1	10.73±1.25	11.85±0.82$^{@}$	9.18±1.04^{y}	9.41±1.82^{y}	0.096±0.0230	0.119±0.0207$^{@}$	0.102±0.0148$^{@}$	0.088±0.0038
BaBG-5	12.43±1.09$^{@,a}$	13.71±0.91$^{@,a,x}$	10.42±0.96^{x,y}	9.82±0.52^{x,y}	0.120±0.0141$^{@}$	0.148±0.0209$^{@,a}$	0.117±0.0091$^{@}$	0.095±0.0106
BaBG-10	15.86±1.31$^{@,a,b}$	16.90±1.19$^{@,a}$	11.14±0.61^{y}	9.25±0.68^{x,y}	0.132±0.0357$^{@,a}$	0.169±0.0258$^{@,a}$	0.121±0.0179$^{@}$	0.098±0.0128^{y}
(v)	Concentration of Ca (ppm) in Kidneys				Concentration of Ba (ppm) in Kidneys			
	D1	D3	D5	D7	D1	D3	D5	D7
Control	93.42±7.89	92.12±4.12	95.19±8.04	97.89±6.43	0.038±0.0041	0.042±0.0063	0.034±0.0048	0.041±0.0069
BaBG-1	98.78±10.82	109.83±2.13$^{@,x}$	94.28±9.15^{y}	95.93±8.45^{y}	0.044±0.0076	0.056±0.0092$^{@,x}$	0.043±0.0070^{y}	0.038±0.002^{y}
BaBG-5	106.13±2.91$^{@}$	118.01±2.24$^{@,x}$	102.59±10.27^{y}	93.50±4.98^{x,y}	0.051±0.0047$^{@}$	0.069±0.0103$^{@,a,x}$	0.050±0.0031$^{@,y}$	0.044±0.0050^{y}
BaBG-10	115.70±6.04$^{@,a}$	132.33±4.08$^{@,a,b,x}$	106.86±5.99$^{@,a,x,y}$	95.57±7.34^{x,y}	0.060±0.0089$^{@,a}$	0.081±0.0116$^{@,a,b,x}$	0.061±0.0064$^{@,a,b,y}$	0.045±0.0028^{x,y,z}
(vi)	Concentration of Ca (ppm) in Spleen				Concentration of Ba (ppm) in Spleen			
	D1	D3	D5	D7	D1	D3	D5	D7
Control	26.18±3.45	25.03±1.89	23.44±2.25	26.12±3.01	0.051±0.0078	0.048±0.0051	0.045±0.0041	0.050±0.0029
BaBG-1	30.67±4.09	37.12±3.58$^{@,x}$	27.84±3.18^{y}	25.78±2.26^{x,y}	0.070±0.0036	0.091±0.0061$^{@}$	0.073±0.0082$^{@}$	0.058±0.0053^{y}
BaBG-5	33.13±4.03$^{@}$	39.93±1.34$^{@,x}$	29.36±1.47$^{@,y}$	24.95±2.01^{x,y}	0.082±0.015$^{@}$	0.147±0.0294$^{@,a,x}$	0.088±0.0162$^{@,y}$	0.060±0.0075^{x,y,z}
BaBG-10	38.26±4.15$^{@,a,b}$	43.09±5.18$^{@,a,x}$	31.21±3.89$^{@,x,y}$	26.41±3.55^{x,y}	0.091±0.025$^{@}$	0.231±0.0336$^{@,a,b,x}$	0.094±0.0102$^{@,y}$	0.062±0.0058^{x,y,z}

(vii)	Concentration of Si (ppm) in Brain			
	D1	**D3**	**D5**	**D7**
Control	0.63±0.055	0.59±0.045	0.61±0.058	0.56±0.071
BaBG-1	0.60±0.045	0.71±0.074$^{@}$	0.68±0.126	0.59±0.070^{y}
BaBG-5	0.67±0.082	0.80±0.093$^{@,x}$	0.71±0.068^{y}	0.62±0.103^{y}
BaBG-10	0.63±0.062	0.88±0.120$^{@,a,x}$	0.68±0.053^{y}	0.65±0.067^{y}
(viii)	**Concentration of Si (ppm) in Lungs**			
	D1	**D3**	**D5**	**D7**
Control	1.46±0.26	1.62±0.13	1.59±0.22	1.48±0.094
BaBG-1	2.67±0.31$^{@}$	3.38±0.25$^{@,x}$	1.92±0.14^{x,y}	1.65±0.23^{x,y}
BaBG-5	2.91±0.28$^{@}$	4.04±0.36$^{@,a,x}$	2.17±0.18$^{@,x,y}$	1.73±0.14^{x,y,z}
BaBG-10	3.12±0.27$^{@,a}$	4.31±0.52$^{@,a,x}$	2.38±0.31$^{@,a,x,y}$	1.71±0.12^{x,y,z}
(ix)	**Concentration of Si (ppm) in Heart**			
	D1	**D3**	**D5**	**D7**
Control	0.83±0.059	0.92±0.172	0.85±0.390	0.89±0.114
BaBG-1	1.49±0.182$^{@}$	1.78±0.161$^{@,x}$	1.23±0.171$^{@,y}$	0.96±0.083^{x,y}
BaBG-5	1.74±0.096$^{@}$	1.96±0.234$^{@}$	1.54±0.201$^{@,a,y}$	1.01±0.160^{x,y,z}
BaBG-10	2.05±0.272$^{@,a,b}$	2.15±0.177$^{@,a}$	1.78±0.103$^{@,a,y}$	1.19±0.184^{x,y,z}
(x)	**Concentration of Si (ppm) in Liver**			
	D1	**D3**	**D5**	**D7**
Control	2.08±0.11	2.17±0.34	2.10±0.16	2.02±0.35
BaBG-1	9.19±1.42$^{@}$	14.08±1.31$^{@,x}$	8.44±1.03$^{@,y}$	3.21±0.47^{x,y,z}
BaBG-5	12.48±1.78$^{@,a}$	19.16±2.62$^{@,a,x}$	10.61±1.76$^{@,y}$	4.01±0.48^{x,y,z}
BaBG-10	17.62±2.49$^{@,a,b}$	24.67±3.26$^{@,a,b,x}$	10.99±2.07$^{@,a,x,y}$	4.96±0.24$^{@,x,y,z}$
(xi)	**Concentration of Si (ppm) in Kidneys**			
	D1	**D3**	**D5**	**D7**
Control	2.51±0.27	2.98±0.31	2.33±0.20	2.80±0.37
BaBG-1	3.61±0.39$^{@}$	8.21±0.66$^{@,x}$	5.03±0.39$^{@,x,y}$	3.04±0.19^{y,z}
BaBG-5	4.01±0.44$^{@}$	11.04±1.34$^{@,a,x}$	6.14±0.48$^{@,a,x,y}$	3.97±0.23$^{@,y,z}$
BaBG-10	6.88±0.71$^{@,a,b}$	14.27±1.45$^{@,a,b,x}$	8.88±0.92$^{@,a,b,x,y}$	4.02±0.46$^{@,a,x,y,z}$
(xii)	**Concentration of Si (ppm) in Spleen**			
	D1	**D3**	**D5**	**D7**
Control	4.71±0.48	4.37±0.30	4.58±0.56	4.19±0.25
BaBG-1	5.42±0.97	9.93±1.64$^{@,x}$	6.02±0.48^{y}	5.03±0.41^{y}
BaBG-5	7.56±0.53$^{@,a}$	13.35±1.16$^{@,a,x}$	8.15±0.97$^{@,a,y}$	5.89±0.83$^{@,x,y,z}$
BaBG-10	10.97±1.51$^{@,a,b}$	17.09±2.31$^{@,a,b,x}$	10.21±1.35$^{@,a,b,y}$	6.61±0.39$^{@,a,x,y,z}$

Data are expressed as mean ± SD (n = 6 male rats/group).$^{@}p<0.05$, $^{a}p<0.05$, and $^{b}p<0.05$ compared to control, 1mg/kg, and 5 mg/kg BaBG b.w. respectively. $^{x}p<0.05$, $^{y}p<0.05$, and $^{z}p<0.05$compared to days after the oral treatment of BaBG (D1, D3, and D5of the individual group respectively). (Two-way ANOVA followed by Bonferroni post-hoc test)

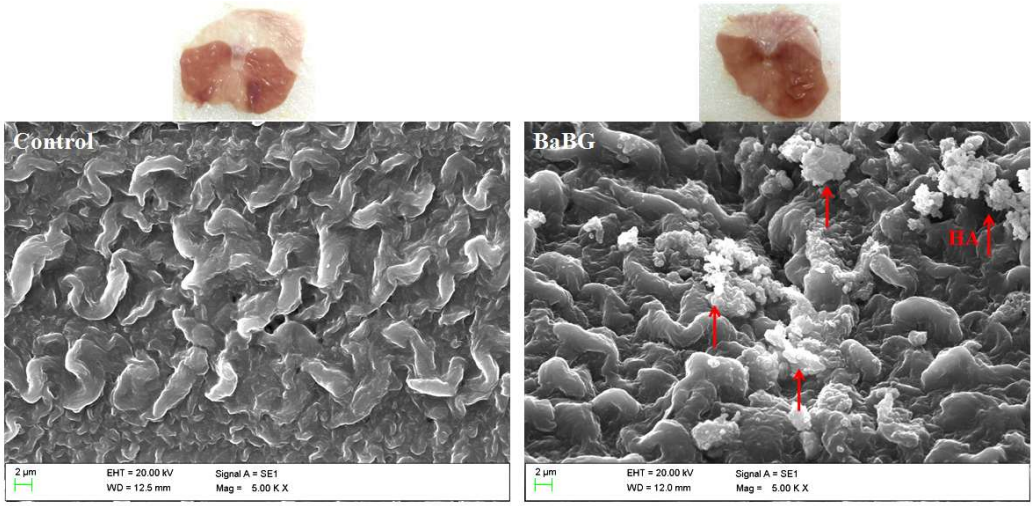

Figure 3.5: Representative scanning electron microscopy image of the stomach of the control and BaBG-treated rat exhibiting the deposition of abundant hydroxyapatite (HA) crystals on the gastric epithelium layer of the stomach without any abrasion of the protective layer qualitatively. The macroscopic photographs of the stomach of both the groups are also showing normal morphology. Magnification: 5k X; scale bars: 2 µm

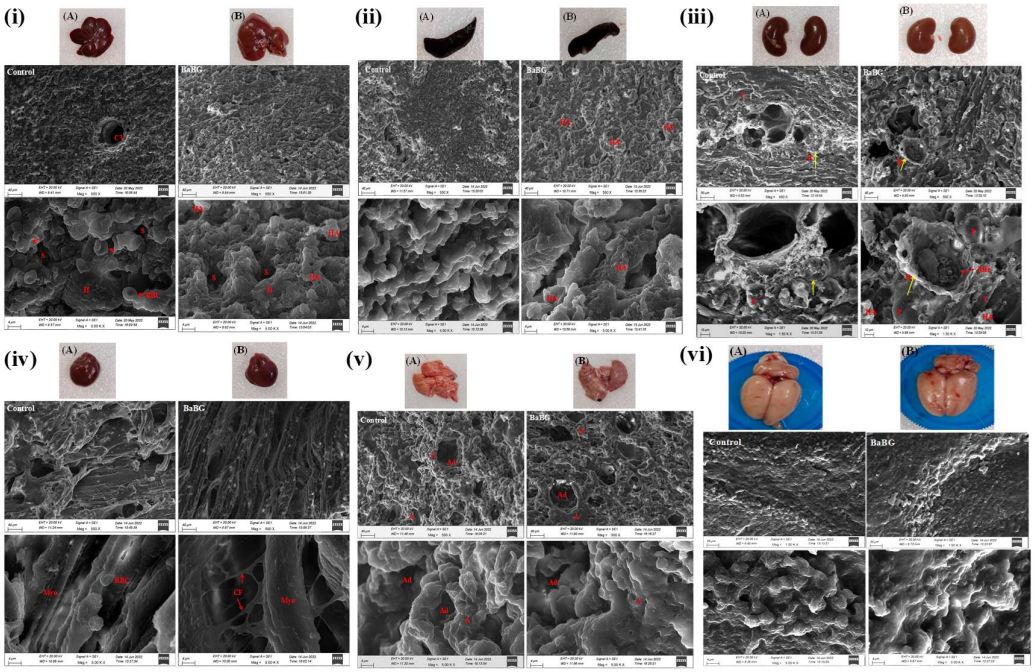

Figure 3.6: Representative photograph of the scanning electron microscopy of liver (i), spleen (ii), kidney (iii), heart (iv), lungs (v), and brain (vi) section of control (A) and orally treated BaBG rat (B). The liver section of the treated rat exhibited the presence of normal hepatocytes (H) surrounding the sinusoids (S) and central vein (CV). The deposition of hydroxyapatite (HA) along with the presence of erythrocytes (RBC; shown in red arrow) is seen. The spleen of BaBG-treated rat exhibiting abundant hydroxyapatite (HA) deposition and the lungs of control and BaBG rats also exhibited

normal alveoli (A) and alveolar duct (Ad). Similarly, the cross-section of the kidneys of treated rat exhibited normal architecture of the Bowman's capsule (B; yellow arrow) along with the glomerular tuft. There are also podocytes (P) and erythrocytes (RBC) visible along with the deposition of crystals of HA. The SEM analysis of heart exhibited intact myofibres (Myo) with the presence of loose connective tissue and collagen fibers (CF). BaBG rats exhibited normal surface morphology in brain section similar to the control rats without any deposition of HA. Magnification of liver, spleen, lung, and heart: 550X and 5 kX; scale bars: 40 µm and 4 µm respectively. Magnification of kidneys: 450 X and 1.5 kX; scale bars: 50 µm and 10 µm respectively. Magnification of brain: 1 kX and 5 kX; scale bars: 20 µm and 4 µm respectively.

3.3. Summary

In the current study, the pre-clinical single-dose oral release kinetics, biodistribution and excretion of dopants from sol-gel derived BaBG were evaluated. BaBG was amorphous and mesoporous in nature and its bioactivity was affirmed by its ability to form HA in SBF. The *in-vitro* release profile for Si, Ca and Ba from the BaBG framework in the simulated physiological milieu exhibited controlled release of the dopants with the maximum concentration observed at 24 h for Ca and Si. Similarly, the *in-vivo* oral pharmacokinetics study demonstrated the dose-dependent release of network modifiers into the plasma and the T_{max} was observed at 24 h for Si, Ca and Ba at all doses. There was dose-dependent elevation in the half-life of Si and Ca and the Vz increased by 4.2 and 4.99-fold respectively at 10 mg/kg. However, the half-life for Ba decreased with an increase in dose. The clearance (CL) of Ba increased 1.90 and 3.11-fold at doses 5 and 10 mg/kg respectively compared to 1 mg/kg BaBG. Further, the excretion study demonstrated feces to be the prime excretory route for Ba and Si. The biodistribution study indicated that Ca, Ba, and Si accumulated mainly in the excretory organs of the body such as the liver, spleen, and kidneys. Moreover, we have observed that barium leached from BaBG was detected in the peripheral organs as well as in the central nervous system i.e., the brain. Therefore, this study provides information on the fate of the released elements from orally administered BaBG, their release pattern, biodistribution and excretion.